

Enhancing As(V) adsorption and passivation using biologically formed nano-sized FeS coatings on limestone: Implications for acid mine drainage treatment and neutralization

Jing Liu¹, Lei Zhou¹, Faqin Dong¹ and Karen A. Hudson-Edwards^{2*}

¹ *The Key Laboratory of Solid Waste Treatment and Resource Recycle, Ministry of Education, Southwest University of Science and Technology, Mianyang, 621010 China.*

² *Department of Earth and Planetary Sciences, Birkbeck, University of London, Malet St., London WC1E 7HX, UK. *Corresponding author. Email: k.hudson-edwards@bbk.ac.uk. Tel: +44-(0)203-073-8030*

Submitted to: *Chemosphere*

Manuscript number: CHEM41980

Date of submission of revised version: 13 October 2016

Keywords: Fe-reducing bacteria, sulfate-reducing bacteria, sorption; arsenic(V); nano; FeS-coated limestone

Abstract

The iron-reducing bacterium *Acidiphilium cryptum* JF-5 and a sulfate reducing bacterium (SRB) collected and purified from the mine drainage of a copper mine in the northwest of Sichuan Province, China, were used to biologically synthesize nano-sized FeS-coated limestone to remove As(V) from solution. The adsorption efficiency of As(V) is improved from 6.64 $\mu\text{g/g}$ with limestone alone to 187 $\mu\text{g/g}$ with the FeS coated limestone in both batch and column experiments. The hydraulic conductivity of the columns are also improved by the presence of the nano-sized FeS coatings, but the solution neutralization performance of the limestone can be reduced by passivation by gypsum and Fe(III) precipitates. Calculations for FeS-coated limestone dissolution experiments show that the process can be described as $n_{\text{Ca,sol}} = At^{1/2} - n_{\text{Ca,gyp}}$. The results suggest that FeS-coated limestone may be an effective medium for remediating As(V)-bearing solutions such as acid mine drainage in systems such as Permeable Reactive Barriers

1. Introduction

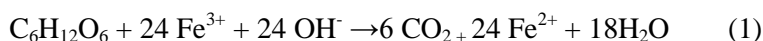
Nano-sized FeS materials offer great potential for removing contaminants due to their superior adsorption performance compared to other minerals (Gong et al., 2016). These reactive FeS materials can be used for treating various contaminants, especially redox-sensitive elements such as arsenic, uranium and chromium. Nano-sized FeS materials not only serve as effective adsorbents, but also as reductants, and they remove the contaminants from waters mainly via chemical adsorption and reductive precipitation.

Permeable reactive barrier (PRB) technology is a widely practiced remediation scheme which treats contaminated groundwater with a permeable wall. Limestone is the most common filling material of PRB, and is used for remediating acid mine drainage (AMD) due to its neutralization ability and low cost (Cravotta and Trahan, 1999; Soler et al., 2008; Liu et al., 2013). However, two potentially negative geochemical issues determine the service time of limestone-filled PRBs. The first relates to the performance of the system. The potential for contaminant adsorption on limestone on contaminants commonly is lower than on other adsorbents such as zero valent iron (Manning et al, 2002, Kanni et al. 2005, Richard et al. 2009, Wilkin et al. 2009) and oxyhydroxysulfate minerals such as schwertmannite. Davis et al. (2007), for example, showed that the adsorption capacity of limestone on As(V) is 0.01 mg/g below pH 8. Kanel et al. (2005) investigated As(III) sorption on zero valent iron at pH 7, and estimated the maximum adsorption capacity to be 3.5 mg/g, whereas Carlson et al. (2002) and Song et al. (2015) both reported maximum adsorption capacities of As(V) on schwertmannite up to 175-183 mg/kg. To improve the adsorption performance, the technology of surface modification has been used. This involves coating the limestone with metal-bearing phases to increase the surface area and improve adsorption. Common coatings used are iron and aluminium hydroxides (Liu et al., 2014b; Henke, 2009). The adsorption of As(V) by aluminium hydroxide coated limestone has been shown to be 0.15 mg/g, which is a significant improvement over the limestone alone (6.6-10.0 µg/g; Liu et al., 2013; Davis et al., 2007; Ohki et al., 1996; Hossain and Islam, 2008).

The second geochemical issue is the passivation of limestone due to the formation of secondary minerals, such as iron hydroxide (Fe(OH)₃) and gypsum (CaSO₄·2H₂O; Soler et al., 2008; Hammack et al., 1994). To prevent this, a reducing layer can be inserted in front of the limestone-filled PRB. This will reduce Fe³⁺_(aq) in AMD to Fe²⁺_(aq) and thus prevent formation of ferric precipitates that will passivate the sys-

tem. This passive treatment is commonly called a reducing and alkalinity producing system (RAPS), and it was previously known as a successive alkalinity producing system (SAPS; Lottermoser, 2010). The reducing layer used is often naturally-occurring organic materials such as mushroom compost Lee et al., 2010) and pea manure (Khan Eusuf Zai et al., 2010). These materials improve the quantity of effluent water and extend the longevity of the PRB, but it is necessary to replace the organic layer monthly or yearly depending on the water chemistry and permeability (Robb and Robinson, 1995; Newcombe and Brennan, 2010) and allow a longer retention time due to bacterial reduction (Lottermoser, 2010).

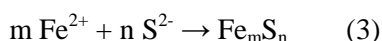
In view of above two issues, a novel biologically-formed FeS-coated limestone was investigated for this study. The nano-sized FeS coating is produced using both Fe-reducing and sulfate-reducing bacteria (*Acidiphilium cryptum* JF-5 and *Desulfovibrio vulgaris miyazaki* SRB, respectively), both of which are common bacteria in AMD Lee et al., 2010; Johnson and Hallberg, 2003). *Acidiphilium cryptum* JF-5 can reduce Fe³⁺ into Fe²⁺ via an enzyme catalyzed reaction, as follows (Küsel et al., 1999):



Sulfate reducing bacteria reduce SO₄²⁻, which is the most common anion in AMD that forms as a product of the oxidation of pyrite (FeS₂). The process can be described as follow:



Thus, biologically formed FeS precipitates can be formed by these two bacteria. The probable chemical reaction is:



Previous research suggests that inorganically-synthesized FeS and FeS-coated sand are likely to improve the performance of limestone-filled PRB systems (Han et al., 2011; Jeong et al., 2011; Renock et al., 2009; Zn and Zhao, 2012). We hypothesize that biologically-formed FeS may also improve this perfor-

mance, as SRB has been shown to result in the removal of metals such as Zn from low pH (3.8 to 4.2) mine waste waters and in the formation of sulfides (Kimura et al., 2006). JF-5 and SRB both survive well in acid environments such as AMD, which is a common type of inlet water that enters limestone-bearing PRBs (Wilmoth, 1974). In addition, Fe^{3+} is a common dissolved ion in AMD and when it precipitates as ferric sulfate precipitates and hydroxides (e.g., schwertmannite, ferrihydrite) the resultant phases can cause clogging of the PRB (Liu et al, 2013; Wang et al., 2014).

Natural and synthetic iron sulfide minerals have been used for immobilizing and capturing arsenic (Renock et al., 2009; Gallegos et al., 2007; Parkman et al., 1999). Renock et al. (2009) synthesized abiotic nanoparticles of Fe_mS_n and mixed these with As(III) in anoxic solutions at pH 5 and 9. They found that the uptake of arsenic in Fe_mS_n resulted in the oxidation of the As-bearing Fe_nS_m to As-bearing greigite (Fe_3S_4), a precursor to pyrite. Mackinawite (FeS), which is inorganically prepared and is used to remove arsenic in groundwater, reduces As(III) into zero-valent arsenic As(0), surface clusters and a realgar (AsS)-like precipitate (Hayes et al., 2009). FeS has also been synthesized by reacting Fe(II) with sulfate produced during biotic sulfate reduction, and this has been shown to be a feasible scheme for the remediation of AMD (Hayes et al., 2009; Zagury et al., 2006; Luptakova and Kusnierova, 2005). In addition, FeS -based systems may have better hydraulic conductivity than systems using zero valent iron (Henderson and Demond, 2013).

However, the potential importance of biotic FeS synthesized using JF-5 and SRB on the performance of limestone-bearing PRBs has not been systematically explored. Such knowledge would benefit the construction of *in situ* biotic PRB systems if the two types of bacteria can be made to flow through the limestone barrier. However, the adsorption capacity of biologically formed FeS on limestone and its neutralization ability need to be determined in the laboratory prior to a field trial. In this paper we report on the capacity of biologically formed FeS -coated limestone and pristine limestone for the adsorption of As(V) and the effects of FeS passivation on neutralization using batch and column experiments. Additionally, the effect of the biologically-formed FeS coating on hydraulic conductivity was investigated. This understanding is essential for the future design and application of *in situ* biologic PRB (ISB-PRB).

2 Materials and methods

2.1 Limestone collection and bacteria culture

Limestone was collected from the strata of the Permian Jialingjiang Formation in Sichuan province, China. The limestone is uniform and micritic. XRD analysis shows that it is composed solely of calcite, with no impurities were discovered at the limit of detection. XRF analysis shows that its chemical composition is $\text{Mg}_{0.1}\text{Ca}_{0.9}\text{CO}_3$.

Acidiphilium cryptum JF-5 is a common iron-reducing bacterium, which was firstly found by Kirsten Küsel. JF-5 grows well in solutions of pH 2.1 to 5.8, which are typical of AMD (Nordstrom, 2011). *Acidiphilium cryptum* JF-5 was kindly provided by Kirsten Küsel of Friedrich Schiller University Jena. The *Acidiphilium cryptum* JF-5 were cultured in 1000 mL of culture media known to be favourable for its growth (Küsel, pers comm., 2015). This media contains 917 mL Tryptone soya broth (Fe-TSB) (0.5 g per 1000 mL), 10 mL glucose (18.016 g per 1000 mL), 70 mL ferric sulfate solution (19.995 g per 1000 mL), 1 mL vitamin solution (100 mg vitamin B₁₂, 80 mg P- amino acid, 20 mg D- biotin, 200 mg niacin, 100 mg Ca-D- Pantothenate, 200 mg aneurin hydrochloride and 300 mg Pyridoxal chloropyramine hydrochloride per 1000 mL, respectively), and 1 mL of a mixed solution of tungstate and selenite (0.5 g NaOH, 3 mg Na₂SeO₃·5·H₂O and 4 mg Na₂WO₄·2 H₂O per 1000 mL, respectively). All of these solutions were sterilized under an ultraviolet lamp.

Sulfate reducing bacteria were collected and purified from the mine drainage of a copper mine in the northwest of Sichuan Province, China. The SRB were enriched and cultivated based on Deutsche Sammlung von Mikroorganismen und Zellkulturen specifications (DSMZ-63) GmbH (German collection of microorganisms and cell cultures) (<http://www.dsmz.de/microorganisms>). The culture solution is composed of three sub-solutions (A, B and C). Solution A was prepared by dissolving 0.5 g K₂HPO₄, 1 g Na₂SO₄, 2 g CaCl₂·2H₂O, 2 g MgSO₄·7H₂O, 2 g DL-Na-lactate, 1 g yeast extract and 1 g Resazurin in 980 mL ultra-pure water. Solution B was prepared by dissolving 0.5g FeSO₄·7H₂O in 10 mL ultra-pure water. Solution C was prepared by mixing 0.1 g ascorbic acid and 10 mL ultra-pure water. Solution A was boiled for several minutes, and then pure N₂ was injected while cooling the solution to room temperature. Solutions A and B were then added to solution C and the pH was adjusted to 7.8. The mixed solution was taken up into a 150 mL inoculation bottle until it become gray-white in colour. The bottle was then sealed and sterilized for 15 minutes at 121°C. When it cooled, 3 mL of the collected SRB bacteria were taken up by

syringe into the mixed solution for inoculation in an anaerobic glove box. The bacteria were cultured for 3-7 days. The culturing of the SRB was considered complete when the solution gave off a rotten egg (hydrogen sulfide) smell.

2.2 Generation and evaluation of the FeS coating

The reaction time of JF-5 and SRB and ratios of these two bacteria cultures are the main factors controlling the quantity of FeS coating. To optimize these factors trial experiments were carried out varying the contact time and ratios of bacteria. 0.5 g of limestone was added to each of three 20 mL crimp top vials. 0.25, 0.5 and 1 mL of culture media with JF-5 was added to the three vials, respectively. An excess of reduced forms of sulfur (S^{2-} or others) was maintained relative to the amount of reduced iron (Fe^{2+}). In other words, the SRB was used to completely reduce S^{6+} (from sulfate) in solution, and different quantities of FeS on limestone were synthesized by respectively adjusting the amount of JF-5 bacteria added and the ageing time. The specific steps are as follow: a constant volume of 18 mL of SRB-generated solution was added to the above three screw cap vials. Afterwards, the vials were placed in an anaerobic glove box to remove O_2 in the vials. The vials were sealed with film, shaken by hand several times, and stored for 3 days (T_1 ; 0.25 mL JF-5 bacteria), 7 days (T_2 ; 0.5 mL JF-5 bacteria) and 7 days (T_3 ; 1 mL JF-5 bacteria), respectively. These three groups of experiments thus represent different ratios of JF5 to SRB and different ageing times, which we regard to be the most important factors determining the performance of FeS in PRB systems. All experiments were carried out in duplicate. The standard deviation from each group of parallel experiment is between 5% and 8%. The resulting supernatants were passed through 0.45 μm filters and analysed for Fe^{2+} and total Fe using the phenanthroline spectrophotometric method (Lenore et al., 1989). The residual FeS coated limestone was digested with 1M HCl and analysed for Fe^{2+} and total Fe. A parallel blank experiment was also carried out to determine the trace concentration of Fe in the HCl.

2.3 As(V) adsorption comparison of pristine limestone and biologically formed FeS coated limestone

2.3.1 Batch adsorption experiments

The preliminary experiments described above informed the development of corresponding batch adsorption experiments. For the latter, 2.00 g of limestone was added to crimp top vials. The JF-5 and SRB bac-

terial solutions ratios which produced the most FeS (1 mL JF-5 and 18 mL SRB) were poured into the vials and different quantities of As(V)-bearing stock solutions (0.1, 0.5, 2.5, 10, 25 and 50 mg/L) were injected in the vials using a pipette. These As(V) stock solutions were prepared from a 1 g/L As(V) stock solution, which in turn was generated by dissolving 4.1644 g sodium arsenate heptahydrate ($\text{Na}_2\text{HAsO}_4 \cdot 7\text{H}_2\text{O}$, Alfa Aesar company) in ultra-pure water. The initial pH values of the 0.1, 0.5, 2.5, 10, 25 and 50 mg/L As(V) stock solutions were adjusted to 2 using 10% v/v HCl.

To investigate the effect of different loads of the biologically-formed FeS on As(V) adsorption, two groups of suspension solutions were kept for 3 and 7 days in an anaerobic glove box, and these were labeled C_1 and C_2 , respectively. Subsequently, the supernatants were passed through 0.45 μm filters, and the residual total As in solution was measured by ICP-OES (iCAP6500 ThermoFisher) to estimate the amount of adsorbed As(V). We appreciate that ICP-OES is not capable of measuring the concentrations of different As species, and reduction of the As(V) to As(III) by the FeS may have occurred during these and our other experiments. We have not measured the speciation of As in the As-sorbed FeS. Therefore, we refer to the post-sorption experiment As as As only, and the pre-experiment As as As(V). All batch experiments with the biologically-formed FeS coatings were carried out in duplicate, and the corresponding standard deviation is shown as error bars in the figures below. Parallel As(V) sorption experiments were also performed with pristine limestone as a control, and these were labelled C_0 .

2.3.2 Column adsorption experiments

To comprehensively evaluate the practicality of treating acidic As-containing waste water with biologically formed nano-sized FeS coatings on limestone, column experiments were carried out. The inside diameter and height of the Plexiglas column were 8.9 and 39.9 cm, respectively. Both ends of the column were covered with nylon netting to avoid the loss of limestone particles. Two water pressures sensors were set on the side of column and connected to a data logger (Campbell Scientific Company, USA) and a computer to record the water pressure and voltage change. The exported voltage was measured using the Loggernet software provided with the data logger, and using the relation between the exported voltage and standard mercury pressure gauge, which has a strong linear relation ($R^2=0.999$) (Supplementary material). The water pressure (Y, psi, 1 psi=0.0689476 bar) has a linear relation with the exported voltage (X, mV)

of $Y=0.975X+0.058$. As these coefficients are implanted in the Loggernet software, the final water pressure can be directly recorded. The columns were filled with coarser-grained limestone (more than 10 mesh) than that used in the batch experiments, to allow observation of the developing hydraulic conductivity and to avoid leakages. The total mass of limestone added to each column was 2.35 kg, the average corresponding pore volume was 750 mL, the column porosity is 43.8% and the linear velocity is 1.0 cm/h. The pore volume of the column was measured by quantifying the volume of water required to saturate the limestone-filled column. A peristaltic pump maintained a constant flow rate of 50 mL/h. The solutions were passed from the bottom to the top of the column to reduce the effects of bubbles produced from the dissolution of limestone on the flow rate. 100 mL effluent samples were collected using a fraction collector. The *in situ* biological FeS coating process was carried out after the limestone grains were packed in the columns. Firstly, 700 mL of the prepared SRB bacteria solution was passed through the limestone-filled column at a constant flow rate of 50 mL/h, and then 500 mL of the JF-5 bacteria solution was flowed through the column at the same flow rate. The system was then aged for 6 days, during which time black precipitates slowly formed (Fig. 1). This *in situ* coating process is regarded to be more practical than using a batch experiment, and to have more potential use in PRB technologies.

The chemical compositions of the solutions used in the column adsorption experiments is 0.5 mg/L As(V) (assumed to be typical of average AMD waters) and 51.6 mg/L SO_4^{2-} , and these were generated from $\text{Na}_2\text{HAsO}_4 \cdot 7\text{H}_2\text{O}$ and Na_2SO_4 . We appreciate that this sulfate concentration is lower than that typically found in AMD waters (usually 100 to 10,000 mg/L; Nordstrom, 2011), but the sulfate in our experiments was used as a sulfur source for the SRB, rather than to simulate AMD. The initial pH of solution was set to 2 using HCl (10% v/v). The pH of the effluent samples was measured with a pH meter (Sartorius Germany PB 21), and these samples were filtered through a 0.45 μm membrane and analyzed for As and Fe by ICP-OES (iCAP6500 ThermoFisher). The column experiment samples were labelled with the prefix C₁ (JF5+SRB). To further understand the difference in performances of FeS coatings produced by different combinations of the bacteria, an additional group of column experiments using only 700 mL SRB solution and 500 mL Fe(II) solution (equivalent to the total mass of iron in C₁ based on calculation of the bacterial culture) were carried out using the same flow sequence. These samples were labelled with the prefix C₂ (SRB+ Fe(II)). A column experiment using pristine limestone was carried out for comparison,

and this was labelled C₀.



Fig. 1. Black FeS coatings formed *in situ* on limestone in column experiments. The FeS in the photo was generated by successively injecting SRB and JF-5 bacterial solutions and ageing the mixture for 6 days.

2.4 Neutralization evaluation

10 g limestone was added to each of two 50 mL centrifugal test tubes. 5 mL of the JF-5 culture media and 50 mL of the SRB culture media were added to these test tubes. The tubes were aged for 3 and 7 days, respectively, based on previous trial and batch experiments, as these times resulted in the production of sufficient biologically formed FeS coatings (approximately 2.1 mg Fe per g limestone) for subsequent work. When the coating process was complete, the supernatant solution was removed by vacuum filtration and the solid mixture, comprising the FeS-coated limestone and suspended FeS particles, was taken up into a glass reactor. 1000 mL of ultra-pure water (18 M Ω Millipore), to which NaNO₃ up to a concentration of 0.01 M was added to create a background electrolyte, was transferred into the reactor. The pH of this solution was adjusted to 2 using dilute H₂SO₄ to create a synthetic acid solution. The dynamic pH variation of suspension was monitored and recorded every 2 minutes with an Automatic Potentiometric Titrator (Met-

ter Toledo T50). The agitation rate was 250 rotations/min and the temperature was controlled at 25°C. Five mL samples of the suspension were collected at 10, 30, 60, 120, 180 and 240 min and passed through a 0.45 µm filter. Their Ca, Mg and Fe concentrations were analysed by ICP-OES to understand the dissolution of the FeS-coated limestone. The two groups of dissolution experiments were labeled with the prefix C₁ (3 days ageing) and C₂ (7 days ageing), and these represent different degree of FeS-coating on limestone. A control experiment using pristine limestone was also performed for 4 h and labeled C₀.

2.5 Sample characterization

Arsenic-adsorbed FeS-coated limestone sample were collected immediately after the conclusion of the batch experiments, and these were subjected to *in situ* infrared spectroscopy using an Attenuated Total Reflection (ATR) Fourier Transform Infrared Spectroscopy (ATR-FTIR, Frontier) with a diamond ATR accessory. Spectra ranging from 400 to 4000 cm⁻¹ were obtained by co-addition of 64 scans with a resolution of 1 cm⁻¹ and a mirror velocity of 0.6329 cm/s. SEM images of these nano-sized FeS particles were obtained by field emission scanning electron microscopy (Zeiss Supra 55). In order to limit oxidation, SEM images were obtained within 2 h after freeze-drying the samples under vacuum conditions for 24 h (cf., Labconco, USA).

Fresh FeS particles were separated from the suspension solution by centrifugation at 10,000 rpm for 5 min (Eppendorf, Centrifuge 5804 R). The particles were washed with O₂-free ultra-pure water, centrifuged at same rate and then freeze-dried under vacuum conditions for 24 h (cf., Labconco, USA). Powder X-ray diffraction (XRD) of the freeze-dried FeS particles was performed on a X'Pert PRO X-ray diffractometer in 2θ mode using CuKα radiation.

3. Results and Discussion

3.1 Evaluation of coating quantity

The mixture of the biologically formed, nano-sized FeS and limestone is termed FeS-coated limestone in this study, due to difficulties in the accurate identification of individual FeS phases. Some of the FeS particles do not coat the limestone, but rather are suspended in solution. The FeS-coated limestone general term we employ is also used more widely for practical applications such as arsenic removal technology

(Sayama et al., 2002; Rashmi et al., 2014).

The amount of FeS coating increases with increasing amounts of JF-5 used in the synthesis and increased duration time of the experiments (Fig. 2). The Fe content in the solid increases by c. 20 times as the addition of JF-5 increases from 0.25 mL to 0.5 mL and the duration time increases from 3 days (T_1) to 5 days (T_2). Between T_2 and T_3 , however, the Fe content in the T_3 solid contains only 3 times more Fe than the T_2 solid. The probable reasons for these variations are the limited Fe source and life cycle of JF-5. Our preliminary study showed that JF-5 grew well when cultured for 5 days and experienced a plateau stage of 2 days based on the optical density and Fe(II) concentration measurement (Supplementary Material Fig. S2). Artificial binding agents such as carboxymethyl cellulose and biopolymers could yield a greater quantity of nano-sized FeS coatings on limestone and improve their stability Cravotta and Trahan, 1999; Gong, 2014; Gong et al., 2012).

The different FeS-coated limestone samples are shown in Fig. 3. The pristine limestone is uniform and composed of microcrystalline calcite. It is creamy yellow-colored, and is often called 'bean curd jelly-like' locally (C_0 in Fig.3). The limestone becomes yellow due to Fe(III) precipitates formed during the treatment of AMD. The FeS-coated limestone is black, and it darkens as the coating thickness increases (see C_1 and C_2 in Fig. 3, corresponding to T_1 and T_2). The size of the FeS particles varies between several 10s of nm and 200 nm in diameter, and the shapes are blocky (Fig. 4). The molar ratio of Fe to S in these precipitates is 2.84:1 based on EDX-SEM elemental analysis of five points on one sample (Fig. S3). Some nano-size FeS particles attach to the JF-5 bacteria (Fig. 4), suggesting that the formation of these FeS particles is related to the activity of JF-5. Most of the XRD diffraction peaks of the black FeS particles match those of mackinawite (PDF024-0073) (Fig. S4). A goethite impurity is also evident, and is attributed to partial oxidation of the FeS, and two peaks at 15-30° 2 θ match those of $(C_{14}H_6N_{20})_n$ which is probably cause by bacterial metabolic activity. In the column experiments, the black precipitates slowly form after injection of the JF-5 bacteria solution, which also suggests that the FeS particles are biologically produced.

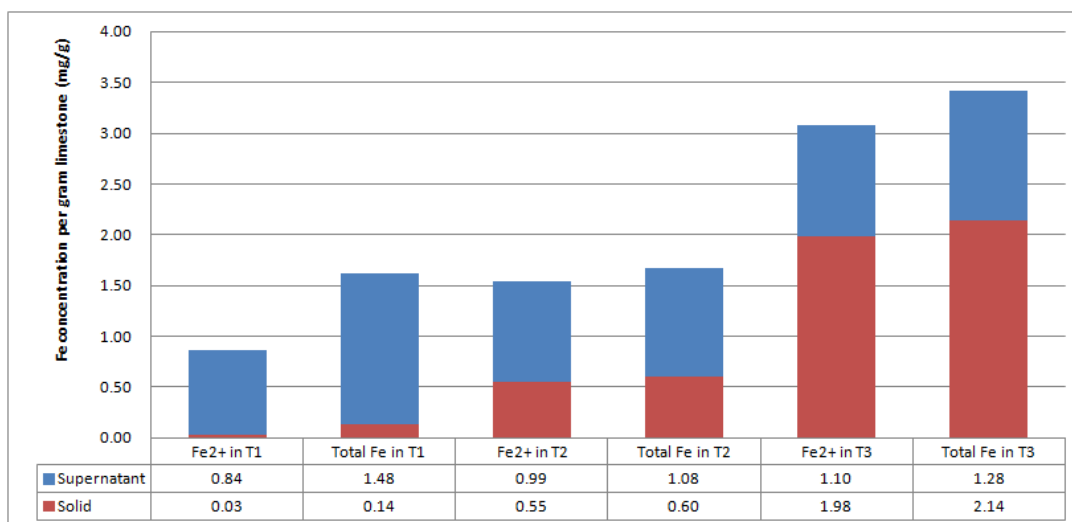


Fig. 2. Fe concentrations/contents in supernatant and limestone (mg/g) for T₁ (0.25 MI JF-5+18 MI SRB, 3days), T₂ (0.5 ml JF-5 +18 ml SRB, 5 days), T₃ (1 mL JF-5 +18 mL SRB, 7 days).

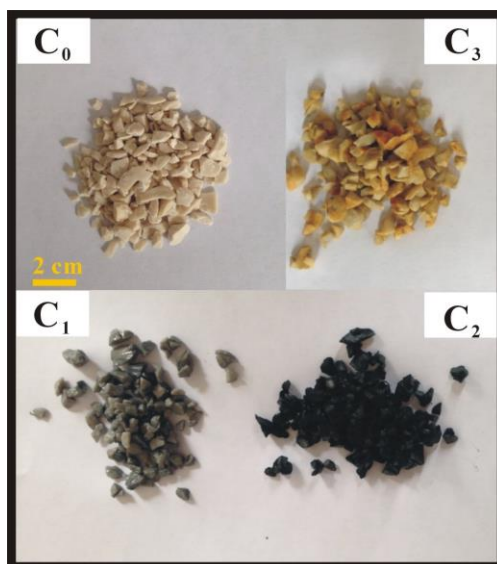


Fig. 3. Photographs of biologically formed FeS-coated limestone. C₀: pristine limestone; C₁: biologically-formed FeS coated limestone aged for 3 days; C₂: biologically-formed FeS-coated limestone aged for 7 days; C₃: pristine limestone reacted with AMD. Scale bar for all photos is 2 cm, as shown in C₀.

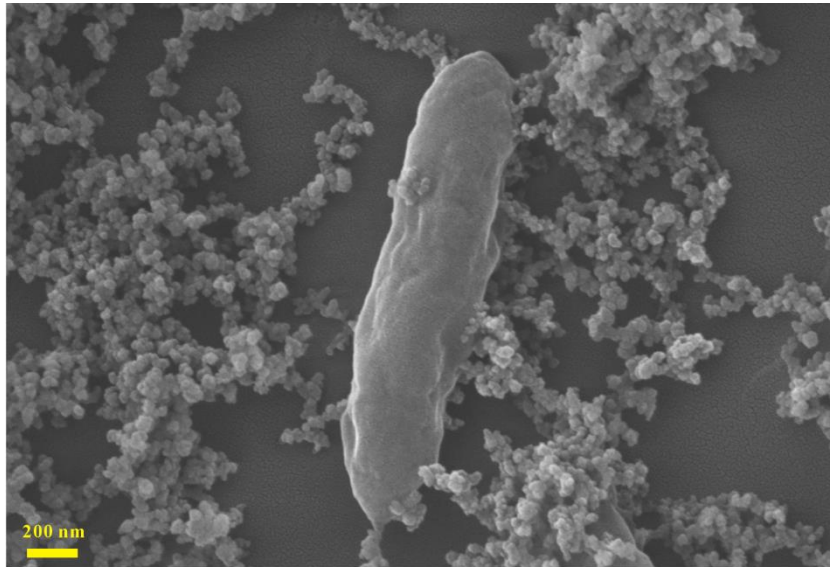


Fig. 4. SEM photomicrograph of nano-sized FeS particles and a JF-5 bacterium.

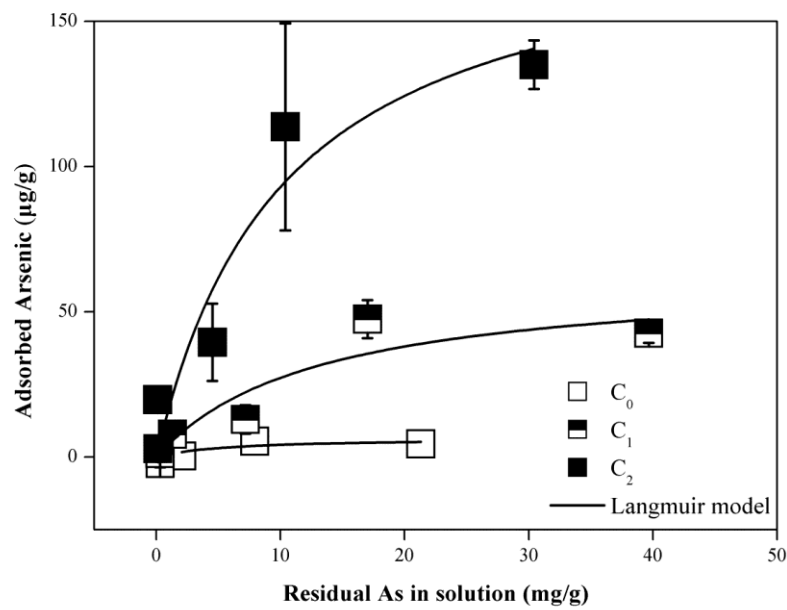


Fig. 5. Isothermal adsorption of pristine and FeS-coated limestone. Error bars represent the standard deviation from the average of two parallel for each batch of biological FeS-coated limestone (C₀: pristine limestone, C₁: 1 mL JF-5 + 18 mL SRB for 3 days, C₂ JF-5 + 18 mL SRB for 7 days; initial pH 5.7).

3.2 Adsorption capacity of FeS-coated limestone

Based on our trial experiments to evaluate the quantity of the FeS coating on the limestone, the ratio of 1:18 for the JF-5 bacterial culture: SRB bacterial culture was chosen for the batch adsorption experiments.

The coating times were set at 3 and 7 days, and these were labelled as C_1 and C_2 , respectively. The maximum As(V) adsorption of pristine limestone is $6.64 \mu\text{g/g}$ (calculated by applying the Langmuir model to the experimental data). This is close to the result of Davis et al. (2007), who reported a maximum adsorption of As(V) on limestone of $10 \mu\text{g/g}$. Once the FeS coating had formed on the limestone for 3 days, its maximum adsorption rapidly increased by 10 times the value of pristine limestone, to $62.9 \mu\text{g/g}$ (C_1 in Fig. 5). The adsorption capacity further increased to $187 \mu\text{g/g}$ when the coating time was extended to 7 days (C_2 in Fig. 5). This increasing adsorption capacity is attributed to the presence of increased amounts of the nano-sized FeS, which likely has a greater surface area and higher adsorption capacity than the limestone alone. Our results are comparable with those of Han et al. (2011), who inorganically synthesized FeS particles on sand, with an average coating of $1.26 \text{ mg FeS / g sand}$ (compared to our $2.14 \text{ mg FeS / g limestone}$). Han et al. (2011) calculated the maximum capacity of coated sand for As(III) (not As(V), as used initially in our experiments) to be 41.7 mg/g FeS at pH 5, but this value is determined by normalizing the data to the amount of the FeS, not to the amount of sand, as we have done in an analogous manner with our limestone. Recalculation of our results to align with those of Han et al. (2011) gives a value of 87.3 mg/g FeS , which is still double the value determined by these authors. The reasons for this discrepancy may be our use of bacteria to generate the FeS, and the different arsenic species used in the two sets of experiments.

3.3 Column transport and hydraulic gradient

Breakthrough curves not only describe the contaminant transport behavior in porous media, but also reflect the retention ability of the media for the contaminants. Breakthrough curve methodologies can help to evaluate the adsorption performance of the filling material in column experiments better than in batch experiments due to the controlled flow rate of the former, especially in large columns (e.g., with 2.35 kg of material in each column). Three breakthrough curves of As(V) in different conditions are shown in Fig. 6. For pristine limestone, the concentration of As(V) in effluent at 2 pore volumes is closed to 0.5 mg/L , which suggests that the column has lost its adsorption capacity. For columns whose FeS coatings were generated with both JF-5 and SRB (C_1 samples), the concentrations of As(V) in effluents at whole measured pore volumes (8) do not exceed 0.1 mg/L , showing the excellent treatment performance of these systems. The differences between the C_1 samples and the C_2 samples (SRB only) were investigated. The re-

duced S species generated by the SRB can directly precipitate with Fe(II) to form a FeS precipitate on the limestone. The results show that the performance of the SRB-generated coatings (C_2 samples) are inferior to those generated by both JF5 and SRB (C_1 samples) (Fig. 6). We do not know the reason for this difference in performance. The FeS particles were uniformly distributed on limestone throughout the column, which further confirms that the potential application of *in situ* biotic PRB is feasible from an operational point of view.

Hydraulic gradients also determine the service time of PRBs. Passivation of the limestone by secondary Fe hydroxides and gypsum is one of main factors resulting in decreases in hydraulic conductivity (Soler et al., 2008; Hammarstrom et al., 2003). In this study, the hydraulic conductivity was assumed to be equal to the difference of water pressure between the top and bottom sensors, and this is attributed to the constant flowing volume for each column provide by the peristaltic pump. The hydraulic conductivity of As(V) transport in the pristine limestone system was better than in the JF5+SRB or SRB-only systems (Fig. 7). This is attributed to the lack of Fe-bearing precipitates in the pristine limestone column and the dissolution of this limestone in the acidic ($\text{pH} = 4$) solutions. The FeS-coated limestone can maintain a very stable hydraulic conductivity. The SRB+Fe(II) column experiment hydraulic conductivities fluctuate considerably in the first stage (when the bacterial solution is injected), reaching values high as 0.70 psi, and this is attributed to the formation of iron-bearing precipitate and to clogging by the bacteria. This rapid clogging is not observed in the column experiments involving solutions from both JF-5 and SRB. Compared to the rapid abiotic formation of FeS (C_2), biologically formed FeS could be more uniformly distributed and require more time to form, and this may help to stabilize the hydraulic gradient. Abiotically-formed FeS-coated limestone also shows stable hydraulic conductivity in the middle and later stages (4000-7800 min), similar to that in the columns with JF-5 and SRB.

Good hydraulic conductivity can be attributed to lack of clogging by secondary phases in a PRB and thus, can improve the long-term service life of the PRB. Pulse flushing and adding organic layers in front of the limestone-filled PRB are methods used in the field to reduce the passivation of the limestone (Cravotta and Trahan, 1999; Caraballo et al., 2009). Existing studies show that precipitation of iron and sulfate ions results in clogging of PRBs (Soler et al., 2008; Liu et al., 2013; Caraballo et al., 2009; Booth et al., 1997). Following on from this, the longevity of PRB has been shown to be inversely related to the

amount of Fe in the system and to the flow rate (Booth et al., 1997). In this study, JF-5 and SRB reduce Fe^{3+} and SO_4^{2-} , respectively, into reduced Fe and S species that form the Fe_nS_m , and this in turn prevents the formation of Fe hydroxides and gypsum. Fe(II)-bearing compounds are more difficult to precipitate, according to the Eh-pH diagram for the Fe-H₂O system (Santomartino and Webb, 2007). Thus, JF-5 theoretically results in the formation of aqueous Fe(II) species that precipitate with reduced S species to form FeS particles, which in turn will benefit hydraulic conductivity. Our column experiments have confirmed this assumption, but further laboratory studies on the hydraulic conductivity and removal performance in the presence of Fe^{3+} , SO_4^{2-} and As(V) need to be carried out to fully elucidate the roles of these ions on PRB efficiency.

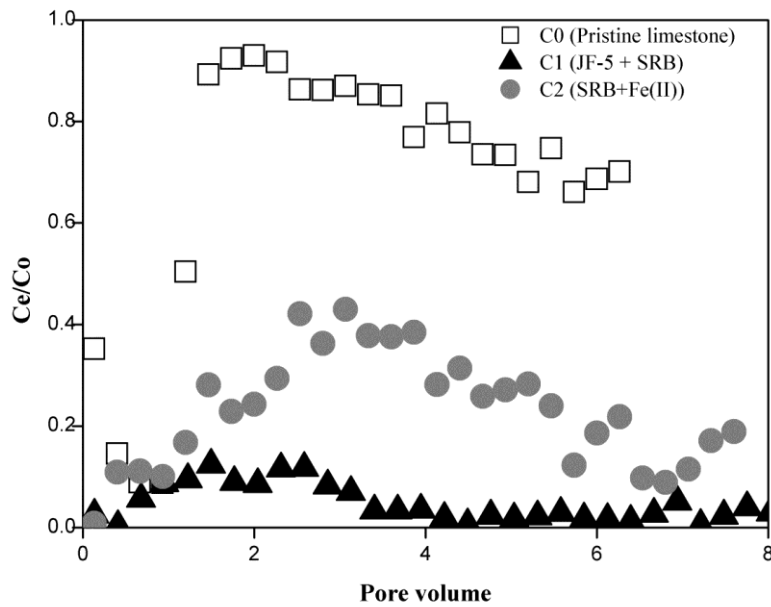


Fig. 6. As(V) breakthrough of As(V) in pristine limestone (C_0) and biologically formed nano-size FeS-coated limestone (C_1 and C_2). C_e/C_0 represents the outlet/inlet As concentrations.

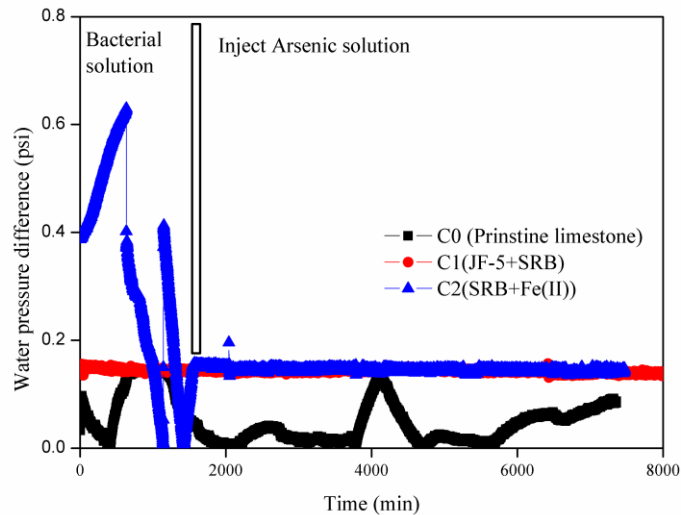


Fig. 7. Hydraulic gradient of three groups of columns (pressure difference = absolute of difference of pressure sensors in the top and bottom, 1 psi = 0.0689476 par).

3.4 Effect of nano sized FeS coating on neutralization capacity of limestone

High concentrations of Fe^{3+} and SO_4^{2-} in AMD often result in the passivation of limestone-filled PRBs by surface precipitates and secondary minerals such as $\text{Fe}(\text{OH})_3$ (ferric hydroxide) and $\text{CaSO}_4 \cdot 2\text{H}_2\text{O}$ (gypsum). Such passivation directly affects the neutralization ability of a PRB. The variation of pH values of the C_0 , C_1 and C_2 solutions is given in Fig. 8. Pristine limestone has the highest neutralisation rate after the first 0.5 h (likely due to the solution being far from saturation), but a pH plateau is experienced before 2 h. The release of Ca into solutions also slows (Fig. 9). The solution pH for C_0 gently increases after 2 h and reaches 7.4 (from the starting pH of 2.2). This rise is attributed to the hydrolysis of CO_3 in solution. Increases in the amount of biological nano-FeS results in slower rates of limestone neutralization over the first 2 h (compare C_1 and C_2 , Fig. 8). The passivation of limestone results in a final pH of 6.3 at the end of the experiment (4 h), which is 1.1 pH lower than in the pristine limestone. This final pH value is nearly same as that due to the hydrolysis of CO_3 in solution, and this should be taken into account in related field studies.

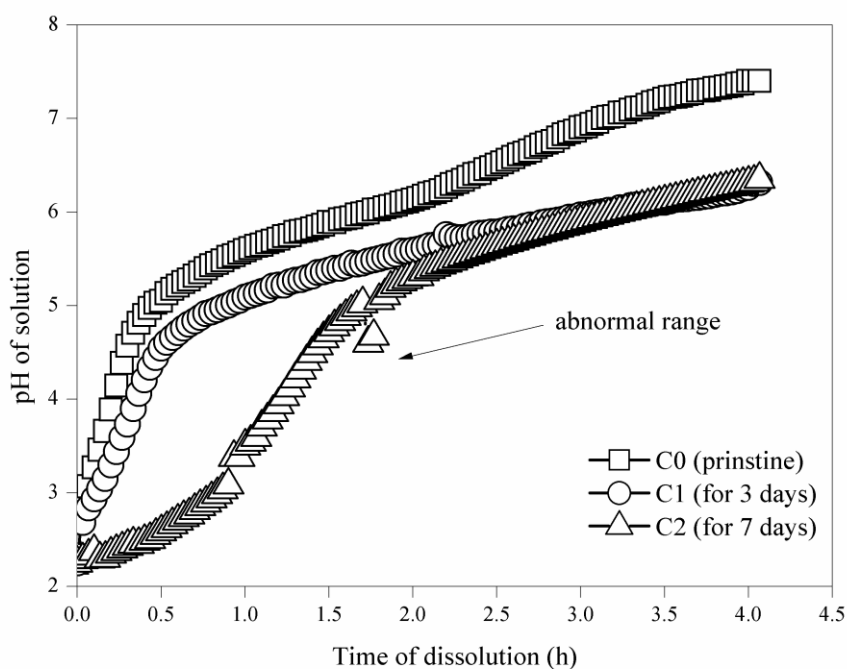


Fig. 8. Effect of biological nano-sized FeS coatings on the neutralization ability of AMD.

In experiment C₂, the solution pH slightly decreased, from 5.01 to 4.74, between 1.69 h and 1.84 h. This was not observed in experiments C₀ and C₁. The explanation for this is the oxidation of FeS coating on limestone, which affects the pH solution. The probable chemical reaction is described as follows:



This proposed reaction is supported the XRD data that suggests that FeS alters to goethite (Fig. S4), and by the aqueous Fe concentrations, which rapidly decrease after 1 h (Fig. S5) while the solution pH is more than 3.2, indicating that iron hydroxides likely begin to precipitate.

Fick's First Law was used to develop a kinetic dissolution model for the limestone (reaction 5). The concentrations of Ca ions along surface normal line of limestone (both pristine and coated limestone) gradually decrease, and can be described by the following formula:

$$J = -D \frac{C_B}{x} \quad (5)$$

In reaction (5), J is the diffusive element flux of limestone per unit area during dissolution, D is the molecular diffusion coefficient, C_B is the concentrations of Ca^{2+} or H^+ ions in the bulk solution and x is the thickness of the FeS coating on the limestone surface. The variation in the thickness of the coating (x) is in turn related to the total moles of Ca released from limestone ($n_{\text{Ca.T}}$), the proportion of gypsum (f_{gyp}) (which takes up released Ca), the porosity of the coating and of the secondary gypsum (ϕ), the uncoated area of limestone (A_R) and the molar volume of the coating (V_m). These relationships can be described by the following reaction, assuming that the surface area of limestone is constant and does not decrease by dissolution:

$$x = \frac{n_{\text{Ca.T}} f_{\text{gyp}} V_m}{A_R (1 - \phi)} \quad (6)$$

The flux of Ca^{2+} from the limestone surface is equal to the half of rate of release of H^+ based on equation (5) so that:

$$\frac{dn_{\text{Ca.T}}}{dt} = -\frac{1}{2} \frac{dn_{\text{H}^+}}{dt} \quad (7)$$

This relationship, and those in equations (5) and (6), can be combined to give an equation describing the rate of Ca release:

$$\frac{dn_{\text{Ca.T}}}{dt} = \frac{DC_{\text{H}^+} A_R (1 - \phi)}{2n_{\text{Ca.T}} f_{\text{gyp}} V_m} \quad (8)$$

This can be integrated to

$$\int_0^{n_{Ca.T}} dn_{Ca.T} = \frac{DC_{H^+} A_R (1-\phi)}{2f_{gyp} V_m} \int_{t_0}^t dt \quad (9)$$

This equals:

$$\frac{n_{Ca.T}^2}{2} = \frac{DC_{H^+} A_R (1-\phi)}{2f_{gyp} V_m} \Delta t \quad (10)$$

Solving for $n_{Ca.T}(t_0=0, t=t)$ gives:

$$n_{Ca.T} = \left(\sqrt{\frac{DC_{H^+} A_R (1-\phi)}{f_{gyp} V_m}} \right) t^{1/2} \quad (11)$$

The constant A can be defined as:

$$A = \sqrt{\frac{DC_{H^+} A_R (1-\phi)}{f_{gyp} V_m}} \quad (12)$$

This allows the total amount of Ca release from the limestone to be calculated as:

$$n_{Ca.T} = At^{1/2} \quad (13)$$

Because the total Ca involves into two parts (dissolved ($n_{Ca.sol}$) and precipitates ($n_{Ca.gyp}$)), equation (13) can be modified to:

$$n_{Ca.sol} = At^{1/2} - n_{Ca.gyp} \quad (14)$$

Therefore, the Ca in solution can be measured, the plot of $n_{Ca, sol}$ and $t^{1/2}$ can be drawn and the corresponding coating model can be built. The resultant dissolution model for pristine and FeS-coated limestone is given in Fig. 9. All of the Ca dissolution data are described very well using this model, as the correlation coefficient is more than 0.90. Based on the estimated $n_{Ca, gyp}$ (19.5 for C₀, 11.3 for C₁ and 16.8 for C₂), it is suggested that a larger volume of secondary gypsum occur on the pristine limestone surfaces than on the FeS-coated limestone.

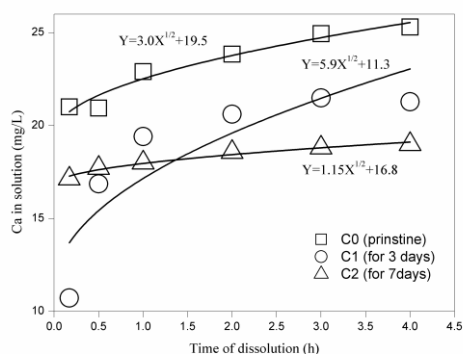


Fig. 9. Calcium release into solution during dissolution of pristine limestone (C₀) and biologically formed nano-size FeS-coated limestone (C₁ and C₂) and their kinetic model based on Fick's diffusion law.

3.5 Mechanism of As removal by biologically formed nano-sized FeS-coated limestone

Attenuated total reflection Fourier-transformation infrared spectroscopy (FTIR) can be used investigate molecular-level surface adsorption. Because the nano-sized FeS is easily oxidized, *in situ* ATR-FTIR of adsorbed As(V) on FeS in supernatant was obtained within 1 h of the experiments (Fig. 10). A free AsO_4^{3-} unit is tetrahedral, which has four fundamental vibrations (Nordstrom, 1997). These include the non-degenerate symmetric stretching mode $\nu_1(A_1)$ at 818 cm^{-1} , the doubly degenerate bending mode $\nu_2(E)$ at 350 cm^{-1} , the triply degenerate antisymmetric stretching mode $\nu_3(F_2)$ at 786 cm^{-1} and the triply degenerate antisymmetric bending mode $\nu_4(F_2)$ at 405 cm^{-1} . Only one weak band at 876 cm^{-1} is observed in the FTIR spectroscopy, however, and the intensity of this band increases with the initial As(V) concentrations used in the experiment. The band is assigned to the symmetric stretching vibration of AsO_4^{3-} , indicating that chemical adsorption may be one of the removal mechanisms. The same position of the FTIR band was observed in the adsorption of As(V) on bone char (Liu et al., 2014a). Another band at 1420 cm^{-1} was ob-

served (Fig. 9), and this is assigned to the ν_3 vibration of CO_3^{2-} . Vibrations at 1638 and 3289 cm^{-1} are attributed to the ν_1 and ν_2 vibrations of liquid water molecular, respectively.

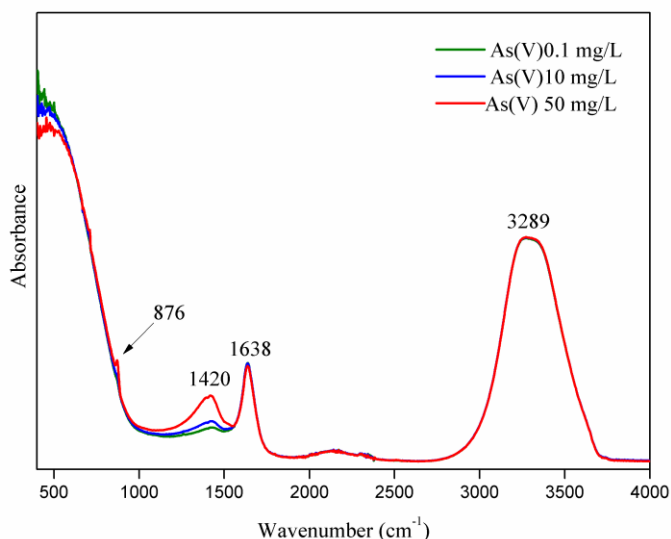


Fig. 10. ATR-FTIR spectra of As(V)-adsorbed FeS-coated limestone for different As(V) initial concentrations.

4. Conclusions

For the first time, JF-5 and SRB have been used to biologically synthesize nano-sized FeS-coated limestone to remove As(V) from solution. Our major findings are that:

- 1) JF-5 and SRB can form nano-sized FeS. The quantity of this FeS coating increases with aging time, and the highest amounts are achieved in seven days;
- 2) biologically formed nano-sized FeS coatings improve the adsorption performance of As(V) on limestone. The maximum adsorption of As(V) is 187 $\mu\text{g/g}$ compared to that for pristine limestone (6.64 $\mu\text{g/g}$). Column experiments also shows nano-sized FeS coated limestone has better retention ability on As(V) than limestone;
- 3) *In situ*, nano-sized FeS on limestone, formed by flowing JF-5 and SRB bacteria through columns, exhibits more stable hydraulic conductivity than FeS formed by Fe(II) and SRB. Nano-sized FeS has a high potential for improving the hydraulic conductivity of PRB systems, especially when influent waters contain high concentrations of Fe(III). It is proposed that nano FeS-coated limestone PRB systems can be

used as a novel alternative for the Successive Alkalinity Producing System;

4) adsorption and hydraulic conductivity are both improved by the nano-sized FeS coatings, but the neutralization ability of the limestone can be reduced by passivation. Dynamic dissolution experiments show that the neutral terminus of the biologically-formed nano-sized FeS coated limestone is 1.1 pH unit lower than that of pristine limestone. The dissolution process of the FeS-coated limestone can be described by the equation $n_{\text{Ca,sol}} = At^{1/2} - n_{\text{Ca,gyp}}$;

5) infrared spectroscopy suggests that chemical adsorption may be one of the removal mechanisms of As(V) by the biologically formed nano-sized FeS.

Acknowledgments

This study was supported by the National Natural Science Foundation of China (Grant 487 No. 41372051). We thank the two anonymous reviewers whose comments greatly helped to improve the manuscript.

References

- An, B., Zhao, D., 2012. Immobilization of As(III) in soil and groundwater using a new class of polysaccharide stabilized Fe–Mn oxide nanoparticles. *J. Hazard. Mater.* 211, 332-341.
- Booth, J., Hong, Q., Compton, R.G., Prout, K., Payne, R.M., 1997. Gypsum overgrowths passivate calcite to acid attack. *J. Colloid Interf. Sci.* 192, 207-214.
- Carlson, L., Bigham, J.M., Schwertmann, U., Kyek, A., Wagner, F., 2002. Scavenging of As from acid mine drainage by schwertmannite and ferrihydrite: a comparison with synthetic analogues. *Environ. Sci. Technol.* 36, 1712-1719.
- Caraballo, M.A., Rötting, T.S., Macías, F., Nieto, J.M., Ayora, C., 2009. Field multi-step limestone and MgO passive system to treat acid mine drainage with high metal concentrations. *Appl. Geochem.* 24, 2301-2311.
- Cravotta, C.A.III., Trahan, M.K., 1999. Limestone drains to increase pH and remove dissolved metals from acidic mine drainage. *Appl. Geochem.* 14, 581-606.
- Davis, A., Webb, C., Dixon, D., Sorensen, J., Dawadi, S., 2007. Arsenic removal from drinking water by

limestone-based material. *Miner. Eng.* 59, 71.

- Gallegos, T.J., Hyun, S.P., Hayes, K.F., 2007. Spectroscopic investigation of the uptake of arsenite from solution by synthetic mackinawite. *Environ. Sci. Technol.* 41, 7781-7786.
- Goldberg, S., C.T. Johnston C.T., 2001. Mechanisms of arsenic adsorption on amorphous oxides evaluated using macroscopic measurements, vibrational spectroscopy, and surface complexation modelling. *J. Colloid Interface Sci.* 234, 204-216.
- Gong, Y., 2014. Immobilization of mercury by carboxymethyl cellulose stabilized iron sulfide nanoparticles: Reaction mechanisms and effects of stabilizer and water chemistry. *Environ. Sci. Technol.* 48(7), 3986-3994.
- Gong, Y., Tang, J., Zhao, D., 2016. Application of iron sulfide particles for groundwater and soil remediation: a review. *Water Res.* 89, 309-320.
- Gong, Y., Liu, Y., Xiong, Z., Kaback, D. Zhao, D., 2012. Immobilization of mercury in field soil and sediment using carboxymethyl cellulose stabilized iron sulfide nanoparticles. *Nanotechnology* 23(29) 294-301.
- Hammack, R., Edenborn, H., Dvorak, D., 1994. Treatment of water from an open-pit copper mine using biogenic sulfide and limestone: a feasibility study. *Water Res.* 28, 2321-2329.
- Hammarstrom, J.M., Sibrell, P.L., Belkin, H.E., 2003. Characterization of limestone reacted with acid-mine drainage in a pulsed limestone bed treatment system at the Friendship Hill National Historical Site, Pennsylvania, USA. *Appl. Geochem.* 18, 1705-1721.
- Han, Y.-S., Gallegos, T.J., Demond, A.H., Hayes, K.F., 2011. FeS-coated sand for removal of arsenic (III) under anaerobic conditions in permeable reactive barriers. *Water Res.* 45, 593-604.
- Hayes, K.F., Adriaens, P., Demond, A.H., Olson, T., Abriola, L.M., 2009. Reduced Iron Sulfide Systems for Removal of Heavy Metal Ions from Groundwater, DTIC Document.
- Henderson, A.D., Demond, A.H., 2013. Permeability of iron sulfide (FeS)-based materials for groundwater remediation. *Water Res.* 47, 1267-1276.
- Henke, K., 2009. Arsenic: Environmental Chemistry, Health Threats and Waste Treatment. John Wiley & Sons, London.

- Hossain, M.S., Islam, M.R., 2008. Experimental and numerical modeling of arsenic transport in limestone. *Energy Sources Pt. A* 30(13), 1189-1201.
- Jeong, H.Y., Han, Y.-S., Park, S.W., Hayes, K.F., 2011. Aerobic oxidation of mackinawite (FeS) and its environmental implication for arsenic mobilization. *Geochim. Cosmochim. Acta* 74, 3182-3198.
- Johnson, D.B., Hallberg, K.B., 2003. The microbiology of acidic mine waters. *Res. Microbiol.* 154, 466-473.
- Kanel, S.R., Manning, B., Charle, L., Choi, H., 2005. Removal of arsenic (III) from groundwater by nanoscale zero-valent iron. *Environ. Sci., Technol.* 39(5), 1291-1298.
- Khan Eusuf Zai, A., Horiuchi, Matsui, T., Meherunnesa, D., 2010. Residual effects of compost and green manure of pea with other organic wastes on nutrient-use efficiency of successive rice after wheat. *Comm. Soil Sci. Plant Anal.* 41, 2154-2169.
- Kimura, S., Hallberg, K.B., Johnson, D.B., 2006. Sulfidogenesis in low pH (3.8-4.2) media by a mixed population of acidophilic bacteria. *Biodegradation* 17, 159-167.
- Köber, R., Welter, E., Ebert, M., Dahmke, A., 2005. Removal of arsenic from groundwater by zerovalent iron and the role of sulfide. *Environ. Sci. Technol.* 39, 8038-8044.
- Küsel, K., Dorsch, T., Acker, G., Stackebrandt, E., 1999. Microbial reduction of Fe (III) in acidic sediments: isolation of *Acidiphilium cryptum* JF-5 capable of coupling the reduction of Fe (III) to the oxidation of glucose. *Appl. Environ. Microbiol.* 65, 3633-3640.
- Lee, S. Kim, S., Jeon, B., Bhatnagar, A., Ji, S., Youngwook, C., Lee, G., 2010. Activity of sulfate reducing bacteria in successive alkalinity producing system: part I-effect of temperature. *Res. J. Chem. Environ.* 14, 67-73.
- Lenore, S., Clesceri, A.E.G., Rhodes, R., 1989. *Trussell Standard Methods for the Examination of Water and Wastewater* (17th edition), American Public Health Association.
- Liu, J., Cheng, H., Zhao, Dong, F., Frost, R.L., 2013. Effect of reactive bed mineralogy on arsenic retention and permeability of synthetic arsenic-containing acid mine drainage. *J. Colloid Interf. Sci.* 394, 530-538.
- Liu, J., Huang, X., Liu, J., Wang, W., Zhang, W., Dong, F., 2014a. Adsorption of arsenic (V) on bone char: batch, column and modeling studies. *Environ. Earth Sci.* 72, 2081-2090.

- Liu, J., Huang, X., Liu, J., Wang, W., Zhang, W., Dong, F., 2014b. Experimental and model studies on comparison of As (III and V) removal from synthetic acid mine drainage by bone char. *Miner. Mag.* 78, 73-89.
- Lottermoser, B.G., 2010. *Mine Wastes: Characterization, Treatment and Environmental Impacts*, Third Edition, Springer, Berlin, Heidelberg, 2010.
- Luptakova, A., Kusnierova, M., 2005. Bioremediation of acid mine drainage contaminated by SRB. *Hydrometallurgy* 77, 97-102.
- Manning, B.A., Hunt, M.L., Amrhein, C., Yarmoff, J.A., 2002. Arsenic(III) and arsenic(V) reactions with zerovalent iron corrosion products. *Environ. Sci. Technol.* 36, 5455-5461.
- Newcombe, C.E., Brennan, R.A., 2010. Improved passive treatment of acid mine drainage in mushroom compost amended with crab-shell chitin. *J. Environ. Engineer.* 136, 616-625.
- Nordstrom, D.K., 1997. Aqueous environmental geochemistry. *Ground Water* 35, 919-920.
- Nordstrom, D.K., 2011. Mine waters: acidic to circumneutral. *Elements* 7, 393-398.
- Ohki, A., Nakayachigo, Naka, K., Maeda, S., 1996. Adsorption of inorganic and organic arsenic compounds by aluminium-loaded coral limestone. *Appl. Organomet. Chem.* 10, 747-752.
- Parkman, R.H., Charnock, J.M., Bryan, N.D., Livens, F.R., Vaughan, D.J., 1999. Reactions of copper and cadmium ions in aqueous solution with goethite, lepidocrocite, mackinawite, and pyrite. *Am. Mineral.* 84, 407-419.
- Rashmi, R.D., Umlong, I.M., Das, B., Borah, K., Thakur, A.J., Raul, P.K., Banerjee, S., Singh, L., 2014. Removal of iron and arsenic(III) from drinking water using iron oxide-coated sand and limestone. *Appl. Water Sci.* 4(2), 175-182.
- Renock, D., Gallegos, T., Utsunomiya, S., Hayes, K., Ewing, R.C., Becker, U., 2009. Chemical and structural characterization of As immobilization by nanoparticles of mackinawite (FeS_m). *Chem. Geol.* 268, 116-125.
- Robb, G.A., Robinson, J.D.F., 1995. Acid drainage from mines. *Geograph. J.* 161, 47-54.
- Santomartino, S., Webb, J.A., 2007. Estimating the longevity of limestone drains in treating acid mine drainage containing high concentrations of iron. *Appl. Geochem.* 22, 2344-2361.

- Sayama, H., Tanaka, S., Ito, M., Machinaga, O., 2002. Calcination process of limestone coated with iron oxide and aluminum oxide. *J. Soc. Inorg. Mat.* 9, 218-223.
- Soler, J.M. Boi, M., Mogollón, J.L., Cama, J., Ayora, C., Nico, P.S., Tamura, N., Kunz, M., 2008. The passivation of calcite by acid mine water. Column experiments with ferric sulfate and ferric chloride solutions at pH 2. *Appl. Geochem.* 23, 3579-3588.
- Song, J., Jia, S.-Y., Ren, H.-T., Wu, S.-H., Han, X., 2015. Application of a high surface-area schwertmannite in the removal of arsenate and arsenite. *Int. J. Environ. Sci. Technol.* 12, 1559-1568.
- Wang, J., Sickinger, M., Ciobota, V., Herrmann, M., Rasch, H., Rösch, P., Popp, J., Küsel, K., 2014. Revealing the microbial community structure of clogging materials in dewatering wells differing in physico-chemical parameters in an open-cast mining area. *Water Res.* 63, 222-233.
- Wilkin, R.T., Acree, S.D., Ross, R.R., Beak, D.G., Lee, T.R., 2009. Performance of a zerovalence iron reactive barrier for the treatment of arsenic in groundwater: Part 1. Hydrogeochemical studies. *J. Contam. Hydrol.* 106, 1-14.
- Wilmoth, R.C., 1974. Limestone and limestone-lime neutralization of acid mine drainage, Mining Pollution Control Branch Industrial Waste Treatment Research Laboratory, U.S. Environmental Protection Agency, Cincinnati, Ohio, 45268, pp. 1-78.
- Zagury, G.J., Kulnieks, V.I., Neculita, C.M., 2006. Characterization and reactivity assessment of organic substrates for sulphate-reducing bacteria in acid mine drainage treatment. *Chemosphere* 64, 944-954.

Supplementary material

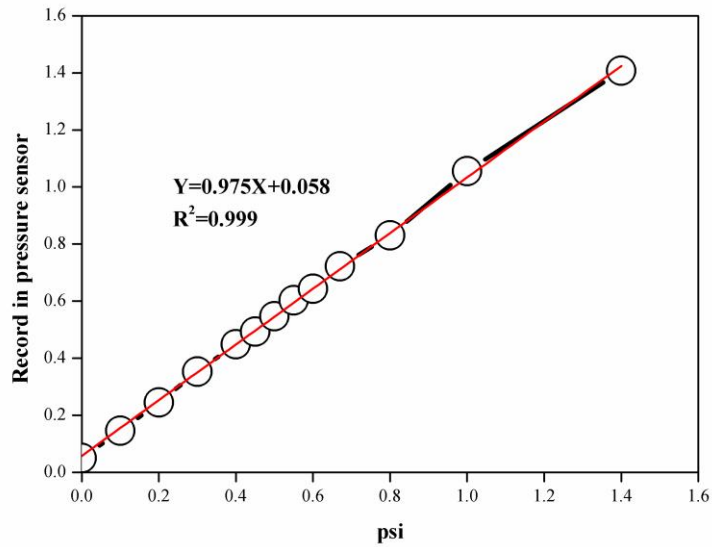


Fig. S1. Calibration of exported voltage and actual pressure.

By measuring the optical density (OD) values and concentration of Fe(II) species in JF-5 bacteria, we are able to understand the growth of JF-5. The OD and concentration of Fe(II) of JF-5 bacteria solution as function of time is shown in Fig. S2. The growth of *A. cryptum* JF-5 basically has reached to stationary phase when cultured in 5-7 days. Ferrous ions are dominant species of iron in solution after 5 days.

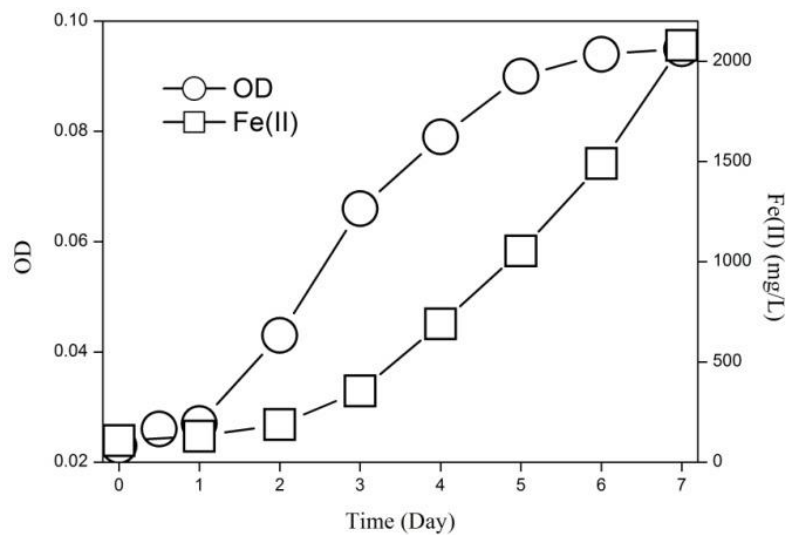


Fig. S2. Growth of JF-5 based on OD and Fe(II) concentrations.

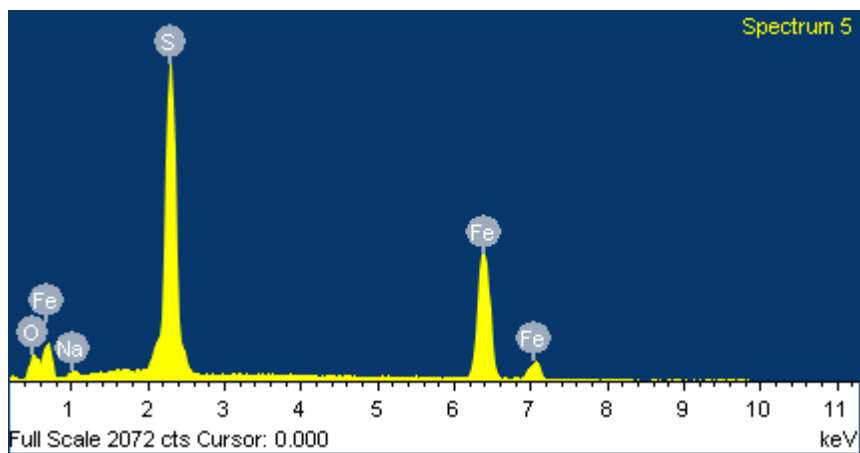


Fig. S3. SEM-EDX of biologically-formed nano-sized FeS precipitates.

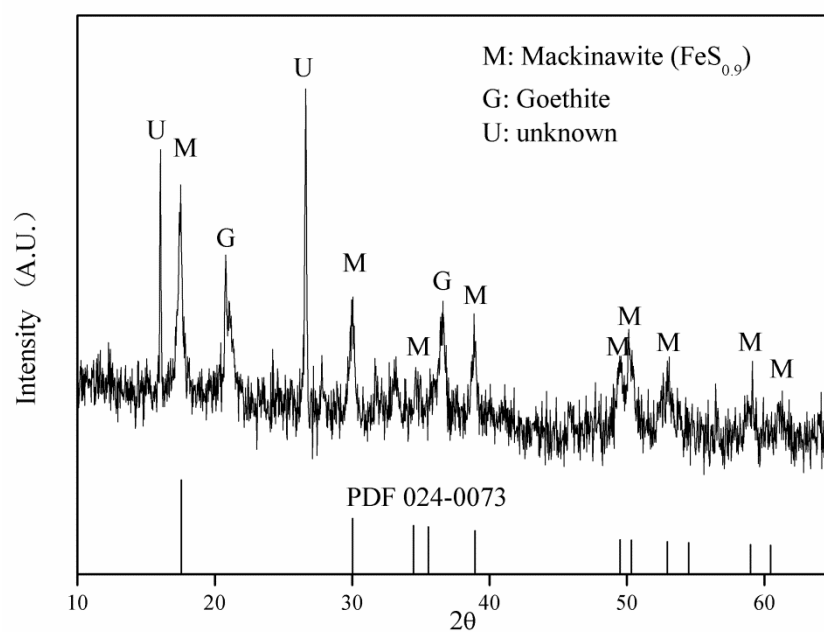


Fig. S4. XRD spectra of black nano-sized particles.

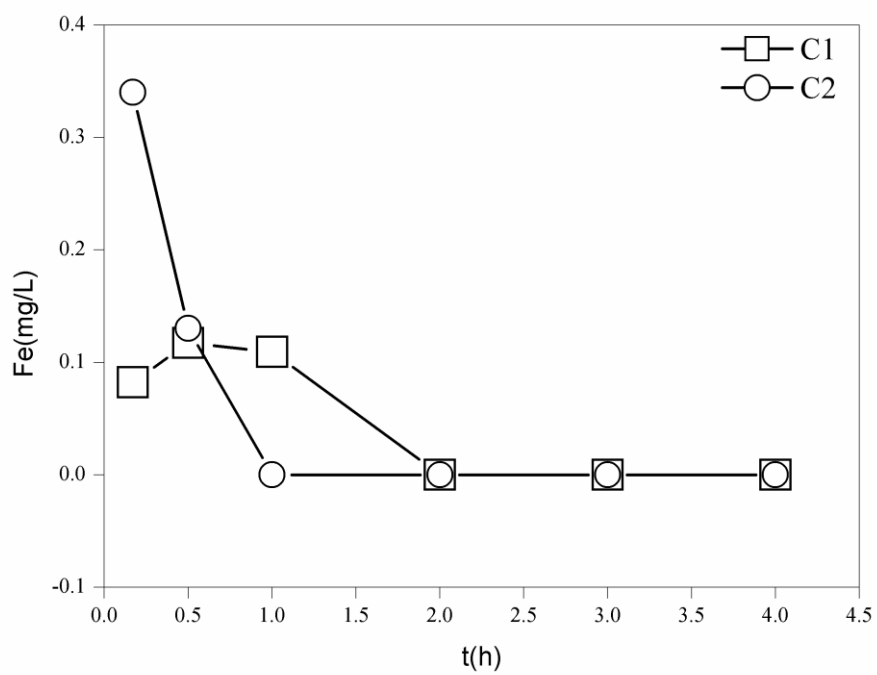


Fig. S5. Iron release of suspension solution with time.